

PAPER • OPEN ACCESS

B2 precipitates formation in Al-containing CoCrFeMnNi-type high entropy alloy

To cite this article: M Klimova *et al* 2021 *IOP Conf. Ser.: Mater. Sci. Eng.* **1014** 012018

View the [article online](#) for updates and enhancements.



240th ECS Meeting ORLANDO, FL

Orange County Convention Center **Oct 10-14, 2021**

Abstract submission deadline extended: April 23rd

SUBMIT NOW

B2 precipitates formation in Al-containing CoCrFeMnNi-type high entropy alloy

M Klimova*, D Shaysultanov, A Semenyuk, S Zhrebtsov, G Salishchev, N Stepanov

Belgorod State University, Belgorod 308015, Russia

*Corresponding author: klimova_mv@bsu.edu.ru

Abstract. The non-equiatomic $\text{Al}_{7.5}\text{Co}_{21.75}\text{Cr}_{5.5}\text{Fe}_{21.75}\text{Mn}_{21.75}\text{Ni}_{21.75}$ high entropy alloy was studied. After cold rolling and annealing at 700-900 °C, a dual-phase ultrafine-grained structure composed of the partially recrystallized fcc matrix and B2 particles was produced; complete recrystallization of the fcc phase was observed after annealing at 1000 °C. The B2 precipitates formation provided a significant strengthening of the alloy in comparison with the single-phase state. The alloy demonstrated an attractive combination of mechanical properties, presenting yield and ultimate tensile strengths of 900 MPa and 1200 MPa, respectively, along with a ductility of 22%.

1. Introduction

A new class of metallic materials, the so-called high-entropy alloys (HEAs), has become a topic of great interest in materials science due to the possibility for attaining unique structures and properties [1]. High-entropy alloys based on 3d transition elements with a face-centered cubic (fcc) structure have demonstrated attractive properties, for example, extremely high ductility and toughness at room and cryogenic temperatures [2]. However, CoCrFeMnNi-based alloys generally have a rather low yield strength at room temperature [3]. The properties of the alloy can be improved by the proper selection of alloying elements along with microstructure modification using thermomechanical treatment, resulting in the formation of an ultrafine-grained recrystallized microstructure [4].

The effect of Al addition to alloys based on Co-Cr-Fe-Ni system has been extensively studied in [5,6]. For example, the as-cast microstructure of FeCoNiCrMn alloys with increasing Al content changed from the initial single fcc structure (until 8 at.% of Al) to a duplex fcc + body-centered cubic (bcc) structure (until 16 at.% of Al) and then to a single bcc structure [7]. However, along with an increase in the strength, a significant drop in the ductility of the Al-containing alloys is observed.

A good strength-ductility combination can be achieved by producing alloys with heterogeneous microstructures, consisting of a soft matrix and hard intermetallic secondary phases [8]. The possibility of B2 strengthening in fcc HEAs based on 3d transition metals was shown in [9,10]. HEAs with dual-phase precipitation-hardened structures can be expected to possess an enhanced balance of mechanical properties. However, the optimal chemical compositions and processing conditions for obtaining proper fcc + B2 microstructures in HEAs is poorly studied. Therefore, the CoCrFeNiMn-type high-entropy alloy, doped by ~7.5 at% of Al was thermomechanically processed to study the effect of Al addition on the microstructure formation and mechanical properties.



2. Materials and Methods

The non-equiatomic $\text{Al}_{7.5}\text{Co}_{21.75}\text{Cr}_{5.5}\text{Fe}_{21.75}\text{Mn}_{21.75}\text{Ni}_{21.75}$ alloy (subscripts indicate the concentration of the respective elements in at.%) was produced using mixtures of pure (≥ 99.9 wt.%) elements by vacuum induction melting. The information on the similar alloy without Al was presented in [11]. The as-cast samples were cold rolled at room temperature to a thickness reduction of 80% and annealed at temperatures of 700–1000 °C for 1 h followed by air cooling. The structure of the alloy was studied by transmission electron microscopy (TEM) using a JEOL JEM-2100 microscope equipped with an energy dispersive spectrometry (EDS) detector and a Nova NanoSem scanning-electron microscope (SEM) with back-scattered electron (BSE) detector and an electron-backscatter-diffraction (EBSD) camera. Samples for SEM and EBSD analysis were prepared by careful mechanical polishing. Samples for TEM analysis were prepared by conventional twin-jet electro-polishing of mechanically pre-thinned 100 μm foils in a mixture of 90% CH_3COOH and 10% HClO_4 at a potential of 30 V at room temperature. Vickers microhardness tests were conducted at room temperature using a load of 300 g. Tensile tests of dog-bone flat specimens (gauge measured $6 \times 3 \times 1.5 \text{ mm}^3$) were performed at room temperature using an Instron 5882 universal testing machine with an initial strain rate of 10^{-3} s^{-1} .

3. Results and Discussion

The alloy in the as-cast condition demonstrated a coarse-grained single-phase microstructure without any secondary phases. The grains had curved irregular boundaries; the average grain size was ~ 150 – $200 \mu\text{m}$. Cold rolling led to the development of a typical for fcc 3d HEAs lamellar-type microstructure formed by twin and (sub)grain boundaries aligned along the rolling direction. Deformation to large strain resulted in a significant strengthening of the alloy; the hardness increased from 165 Hv in the as-cast condition to 385 Hv after 80% thickness reduction.

The effect of cold-rolling and annealing at 700–1000 °C for 1 h on the microstructure of the Al-containing CoCrFeNiMn alloy is shown in Figure 1. Thermomechanical processing resulted in the recrystallization of the matrix and the precipitation of second-phase particles. After annealing at 700 °C, a partially recrystallized structure consisted of deformed areas and regions with fine recrystallized grains was observed. An increase in the annealing temperature to 800 °C and 900 °C led to the further development of the primary recrystallization (Figure 1b, c), characterized by a gradual increase in the recrystallized volume fraction and grain size. The completely recrystallized structure was formed after annealing at 1000 °C (Figure 1d).

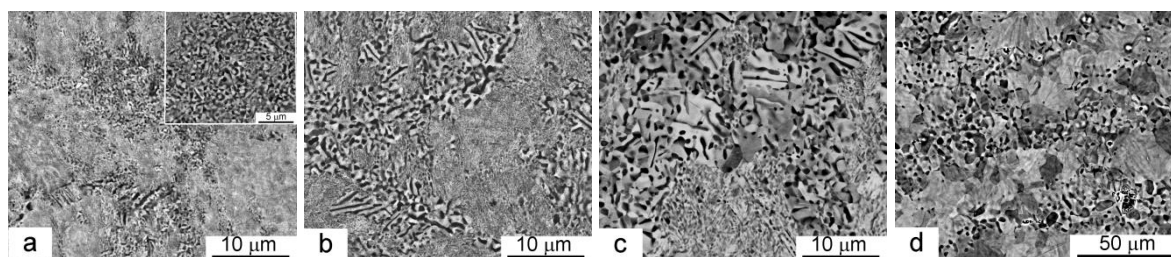


Figure 1. SEM-BSE images of the microstructure of the Al-containing CoCrFeMnNi-type alloy after annealing at 700 °C(a), 800 °C (b), 900 °C (c), 1000 °C (d).

The high magnification image (shown in Figure 1a) showed that the formation of precipitates occurred in the recrystallized regions. It is worth noting that the particles had both lamellar and close to equiaxial morphology. An increase in the annealing temperature was characterized by a rise of the fraction of equiaxed particles. The coarsening of the particles correlated with decreasing their volume fraction in the recrystallized areas during annealing. A gradual increase in the particles' transverse size from 190 nm to 660 nm along with a reduction of the fraction of particles from 33% to 7% were observed with increasing the annealing temperature from 700 °C to 1000 °C (Figure 2a).

The average size of the recrystallized grains of the alloy (Figure 2b) slightly increased from 0.9 μm to 1.5 μm when the annealing temperature changed from 700 $^{\circ}\text{C}$ to 900 $^{\circ}\text{C}$. At the same time, a further increase in the annealing temperature to 1000 $^{\circ}\text{C}$ resulted in a significant rise of the grain size to 5.5 μm . Most likely, the precipitation of second-phase particles inhibited the grain growth in the Al-containing alloy (compare with the single-phase CoCrFeMnNi-type alloy [11] in Figure 2b) resulting in the formation of an ultrafine-grained matrix. Note that no secondary phases were found in the CoCrFeMnNi-type alloy without aluminum after the same annealing temperatures 700-1000 $^{\circ}\text{C}$ [11].

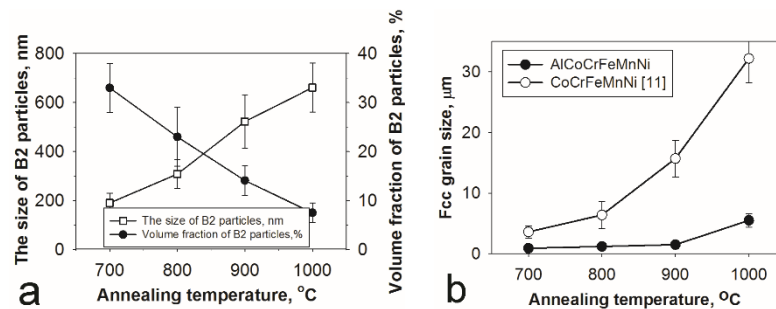


Figure 2. Dependencies of the size and volume fraction of B2 particles (a) and the fcc grain size (b) of the Al-containing CoCrFeMnNi-type alloy on annealing temperature.

A typical EBSD map (Figure 3a,b) of the Al-containing alloy demonstrated a dual-phase microstructure, consisting of the fcc matrix and particles with a bcc crystal structure. In addition, two peaks were found in the distribution of misorientation angles (insert on Figure 3b). The results of orientation image microscopy showed orientation relationship between the matrix grains and the particles corresponding to the Kurdjumov-Sachs OR: $\{111\}_{\text{fcc}} // \{110\}_{\text{bcc}}$ and $\langle 110 \rangle_{\text{fcc}} // \langle 111 \rangle_{\text{bcc}}$ (fcc/bcc misorientation of $\sim 45^{\circ}$). The $\Sigma 3$ boundaries (twin/matrix misorientation of 60°) indicated the presence of numerous annealing twins in the structure. The TEM microstructure of the alloy is presented in Figure 3c. The superlattice reflections $\{100\}$ in the SAED pattern from the $[001]$ bcc zone axis (Figure 3d) indicate the ordering of the BCC lattice, i.e., the particles had a B2 type structure. The EDS chemical analysis revealed that the B2 intermetallic phase was rich in Al and Ni.

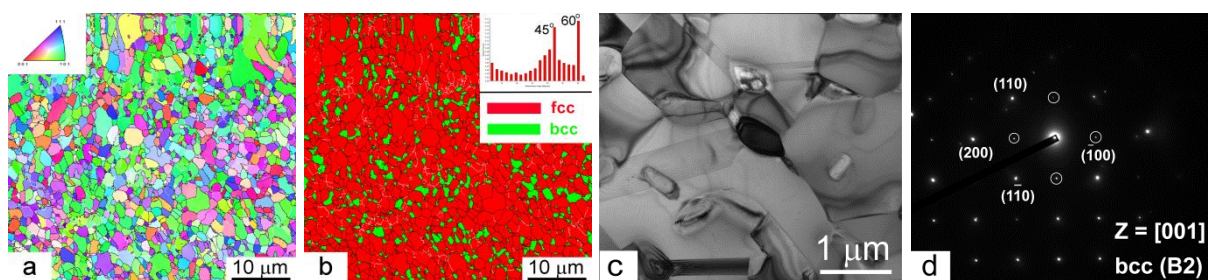


Figure 3. IPF map (a) and corresponding phase map (b); TEM bright-field image (c) and corresponding SAED pattern obtained from $[001]$ B2 zone axis (d) of the Al-containing CoCrFeMnNi-type alloy after annealing at 900 $^{\circ}\text{C}$.

The formation of a dual-phase precipitation-hardened fcc + B2 structure due to the addition of Al to the CoCrFeMnNi alloy provided a considerable increment in strength. The Al-containing CoCrFeMnNi-type alloy demonstrated higher values of microhardness compared to the undoped single-phase HEA [11] after the same thermomechanical treatment (Figure 4a). The Al-containing alloy in the as-cast condition with a single-phase coarse-grained structure exhibited a rather low yield strength of 220 MPa along with a high ductility of 68% (Figure 4b). Cold rolling followed by annealing resulted in a significant strengthening and some reduction of elongation to fracture of the alloy. For example,

annealing at 700 °C provided a high yield strength of 1160 MPa and an ultimate tensile strength of 1500 MPa, but the hardening capacity of the alloy was quite limited. An acceptable ductility of 22% was achieved at the expense of the strength of the alloy: yield strength and ultimate tensile strength of 900 MPa and 1200 MPa, respectively, were obtained after annealing at 800 °C. A further increase in the annealing temperature led to softening and enhancement of the ductility of the alloy.

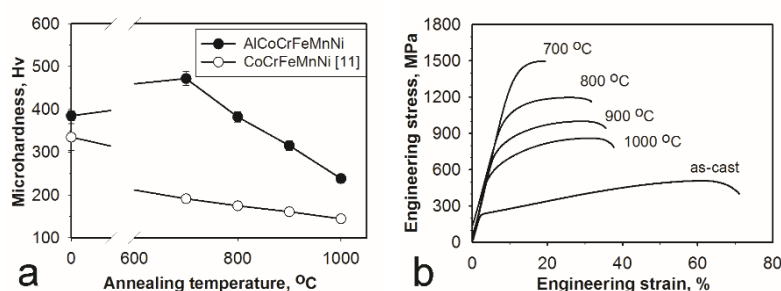


Figure 4. Microhardness (a) and tensile stress-strain curves (b) of the Al-containing CoCrFeMnNi-type alloy after cold rolling and annealing at different temperatures.

4. Conclusions

In summary, the microstructure evolution and mechanical properties of the Al-containing CoCrFeNiMn-type high-entropy alloy subjected to cold rolling followed by annealing at 700-1000 °C were studied. The presented results demonstrated that the addition of 7.5 at.% of Al to the CoCrFeMnNi alloy resulted in the fcc + B2 microstructure formation via thermomechanical processing, which provided a very attractive combination of strength and ductility.

Acknowledgements

The authors gratefully acknowledge the financial support from the Russian Science Foundation Grant No. 18-19-00003. The authors are grateful to the personnel of the Joint Research Center, «Technology and Materials», Belgorod State University, for their assistance with instrumental analysis.

References

- [1] Yeh J-W, Chen S-K, Lin S-J, Gan J-Y, Chin T-S, Shun T-T, Tsau C-H and Chang S-Y 2004 *Adv. Eng. Mater.* **6** 299
- [2] Gludovatz B, Hohenwarter A, Catoor D, Chang E H, George E P and Ritchie R O 2014 *Science* **345** 1153
- [3] Gali A and George E P 2013 *Intermetallics* **39** 74
- [4] He J Y, Wang H, Huang H L, Xu X D, Chen M W, Wu Y, Liu X J, Nieh T G, An K and Lu Z P 2016 *Acta Mater.* **102** 187
- [5] Wang W R, Wang W L, Wang S C, Tsai Y C, Lai C H and Yeh J W 2012 *Intermetallics* **26** 44
- [6] Yang T, Xia S, Liu S, Wang C, Liu S, Zhang Y, Xue J, Yan S and Wang Y 2015 *Mater. Sci. Eng. A* **648** 15
- [7] He J Y, Liu W H, Wang H, Wu Y, Liu X J, Nieh T G and Lu Z P 2014 *Acta Mater.* **62** 105
- [8] Sathiyamoorthi P and Kim H S 2020 *Prog. Mater. Sci.* 100709
- [9] Dasari S, Jagetia A, Chang Y J, Soni V, Gwalani B, Gorsse S, Yeh A C and Banerjee R 2020 *J. Alloys Compd.* **830** 154707
- [10] Lozinko A, Zhang Y, Mishin O V, Klement U and Guo S 2020 *J. Alloys Compd.* **822** 153558
- [11] Klimova M, Shaysultanov D, Semenyuk A, Zherebtsov S and Stepanov N 2021 *J. Alloys Compd.* **851** 156839